aires would succeed in preventing slash-and-burn farming in 70% of the concession. For further details, see (*17*).
22. M. C. Hatchwell, personal communication.
23. Figures are rounded in the text to avoid false precision.
24. D. M. Wolfire, J. Brunner, N. Sizer, *Forests and the Democratic Republic of Congo* (World Resources Institute, Washington, DC, 1998).
25. J. Brunner, K. Talbott, C. Elkin, *Logging Burma's Frontier Forests: Resources and the Regime* (World Resources Institute, Washington, DC, 1998); see also references in (*18*).
26. We used Geographic Information System (GIS) to determine if road-building costs or transport costs limit access to particular areas. A cost-surface, calculated as the total distance to the nearest existing road or port multiplied by the cost per kilometer of building new roads and transporting timber, was consistently offset by the financial benefits of harvesting the timber up to 50 km; thus, no constraints operated within an area the size of the Masoala Peninsula (~4000 km^2). See also (*17*).
27. S. Fankhauser, *Valuing Climate Change: The Economics of the Greenhouse* (Earthscan, London, 1995). For the year 1995, 50% of simulation runs estimated an optimal carbon tax >$20/t C, and optimal tax levels associated with a given probability increased each year [T. Roughgarden and S. H. Schneider, *Energy Policy* **27**, 415 (1999)].
28. Net committed emissions take into account the total weighted emissions of greenhouse gases over time from deforestation and the uptake of gases due to regrowth, and are calculated in CO_2 C equivalents that account for varying greenhouse gas potentials and ratios of different gases. We assumed that burning a hectare of primary rain forest, with reburns every ~3 years, would result in the net release of ~191 metric tons of CO_2 C equivalents [P. M. Fearnside, *Climatic Change* **35**, 321 (1997)]. We further assumed that release of carbon would be amortized over 10 years. Due to the time value of money, this timed release reduced the NPVs of greenhouse gas conservation by ~1.8 times.
29. R. Mittermeier, N. Myers, J. Thomsen, *Conserv. Biol.* **12**, 516 (1998).
30. R. Schawarze [*Ecol. Econ.* **32**, 255 (2000)] found an average cost per ton of CO_2 of $2.6 for land use, cover change, and forestry projects; see S. Brown *et al.* in (*5*).
31. Population Reference Bureau, "World Population Data Sheet 1995" (Population Reference Bureau, Washington, DC, 1997).
32. Although the best management practices scenario generates similar opportunity costs, it would be more difficult for Madagascar to implement than simple protection of the forest [see I. A. Bowles *et al.* in (*21*)], and therefore less likely to prevent deforestation reliably and to obtain carbon credits (*36*); nor would it provide the biodiversity benefits of strict conservation [J. Robinson, *Conserv. Biol.* **7**, 20 (1993)].
33. For example, semi-arid savannahs [B. Walker, *Envir. Dev. Forum* **4**, 204 (1999); see also references in (*18*)].
34. J. O. Niles and R. Schawarze, in *Proceedings of the IEA Bioenergy Task25 Workshop: Bioenergy for Mitigation of CO_2 Emissions: The Power, Transportation and Industrial Sectors*, K. Robertson and B. Schlamadinger, Eds. (International Energy Agency, Graz, Austria, 2000).
35. S. H. Schneider, *Climatic Change* **39**, 1 (1998).
36. Preventing deforestation is an emission reduction, whereas planting trees is a sequestration process. Currently, conserving forests has stronger legal status under the Clean Development Mechanism because it is an emission reduction. The Kyoto Protocol requires verification of real, measurable, voluntary, and long-term reductions. Costa Rica has evolved strategies for dealing with leakage and additionality [D. C. Goldberg, R. Castro, S. Mack, "Carbon conservation: Climate change, forests and the Clean Development Mechanism" (Center for International Law, Centro de Derecho Ambiental y de los Recursos Naturales, Washington, DC, 1998)]. Ultimately, however, industrialized countries will also have to reduce their own emissions in order to meet the goals of the United Nations Framework Convention on Climate Change.
37. R. A. Kramer, D. D. Richter, S. Pattanayak, N. P. Sharma, *J. Environ. Manage.* **49**, 277 (1997).
38. H. J. Ruitenbeek, *Ecol. Econ.* **6**, 57 (1992)
39. We are grateful to C. Ramilison, I. Raymond, R. Lemaraina, B. Simeone, B. Delaite, and M. Hatchwell for providing pricing information and unpublished reports. We thank K. Chomitz, N. Myers, B. Delaite, P. Frumhoff, J. Hardner, G. Heal, J. Hellman, L. Goulder, J. McNeely, J. Paddack, D. Rice, R. Schawarze, S. Schneider, and P. Vitousek for discussions and/or critical readings of the manuscript. The Center for Conservation Biology, the Wildlife Conservation Society, the Heinz Foundation, and the Morrison Institute for Population and Resource Studies supported the authors during this work. We appreciate the assistance of the Masoala Project, run by CARE International Madagascar and Wildlife Conservation Society under the guidance of the Direction des Eaux et Forets and the Association pour la Gestion des Aires Protégées.

6 December 1999; accepted 14 February 2000

mGluR1 in Cerebellar Purkinje Cells Essential for Long-Term Depression, Synapse Elimination, and Motor Coordination

Taeko Ichise,[1] Masanobu Kano,[2,3] Kouichi Hashimoto,[2,3] Dai Yanagihara,[2,4,5] Kazuki Nakao,[1] Ryuichi Shigemoto,[2,6] Motoya Katsuki,[1,2] Atsu Aiba[1]*

Targeted deletion of metabotropic glutamate receptor–subtype 1 (mGluR1) gene can cause defects in development and function in the cerebellum. We introduced the mGluR1α transgene into mGluR1-null mutant [mGluR1 (–/–)] mice with a Purkinje cell (PC)–specific promoter. mGluR1-rescue mice showed normal cerebellar long-term depression and regression of multiple climbing fiber innervation, events significantly impaired in mGluR1 (–/–) mice. The impaired motor coordination was rescued by this transgene, in a dose-dependent manner. We propose that mGluR1 in PCs is a key molecule for normal synapse formation, synaptic plasticity, and motor control in the cerebellum.

mGluRs are G protein–coupled glutamate receptors and are implicated in modulation of synaptic transmission and plasticity (*1*). mGluR1 (−/−) mice have characteristic cerebellar symptoms such as ataxic gait, intention tremor, and motor discoordination (*2–4*). The blockade of mGluR1 by antiserum to mGluR1 results in ataxia, suggesting that mGluR1 is required for motor coordination (*5*). In mGluR1 (−/−) mice, the anatomy of the cerebellum, the morphology of PCs, and the synaptogenesis onto PCs from parallel fibers (PFs) are normal. However, developmental transition from multiple to mono-innervation of PCs by climbing fibers (CFs) (*6*), the other excitatory input to PCs (*7*), is impaired during the third postnatal week (*8*). Long-term depression (LTD) at PF-PC synapses is clearly deficient in mGluR1 (−/−) mice (*3*, *4*). Thus, mGluR1 is thought to be essential for CF synapse elimination and LTD induction, and its disruption may contribute to motor deficits of mGluR1 (−/−) mice. However, mGluR1 is expressed in various cell types in the central nervous system (CNS) other than PCs. Hence it is not clear to what extent mGluR1 in PCs contributes to these phenotypes.

We introduced a transgene (L7-mGluR1) that expressed mGluR1α under the control of the PC-specific L7 promoter (Fig. 1, A and B) into the mGluR1 (−/−) mice. One line of transgenic mice homozygous mutant for endogenous mGluR1 allele showed the cerebellum-restricted expression of the transgene (Fig. 1C) (*9*). (We refer to these mice as mGluR1-rescue mice.) The amount of mGluR1α protein in mGluR1-rescue cerebella was about 80-fold less than that in wild-type cerebella (Fig. 1C). mGluR1α immunoreactivity was abundant in the cerebellum, olfactory bulb, and thalamus in wild-type mice, whereas it was restricted to the

[1]Laboratory of DNA Biology and Embryo Engineering, Center for Experimental Medicine, Institute of Medical Science, University of Tokyo, Tokyo 108-8639, Japan. [2]Core Research for Evolutional Science and Technology (CREST), [3]Department of Physiology, School of Medicine, Kanazawa University, Kanazawa 920-8640, Japan. [4]Toyohashi University of Technology, Toyohashi 441-8580, Japan. [5]Brain Science Institute, RIKEN, Wako 351-0198, Japan. [6]Laboratory of Cerebral Structure, National Institute for Physiological Sciences, Myodaiji, Okazaki 444-8585, Japan.

*To whom correspondence should be addressed: E-mail: aiba@ims.u-tokyo.ac.jp

cerebellum in mGluR1-rescue mice (Fig. 1E) (*10*). High-magnification micrographs revealed that mGluR1α was selectively localized in dendrites of PCs in mGluR1-rescue mice. mGluR1-rescue mice showed no ataxic gait or tremor and could walk along a straight line as do wild-type littermates (Fig. 1D). However, because mGluR1-rescue mice got more excited than wild-type mice when their tails were grasped, the experimenter easily recognized mGluR1-rescue mice without knowing their genotype. This hyperexcitability was similar to that of mGluR1 (−/−) mice.

We asked whether CF synapse elimination could be restored by introducing the mGluR1α transgene (*11*). When a CF was electrically stimulated, a clearly discernible excitatory postsynaptic current (EPSC) was elicited in an all-or-none fashion in the majority of wild-type and mGluR1-rescue PCs (Fig. 2, A and E, upper traces) and in about 40% of mGluR1 (−/−) PCs (Fig. 2C, upper trace). In the remaining PCs, more than one discrete CF-EPSC was elicited at different stimulus sites or at one stimulus site with different stimulus thresholds (Fig. 2, A, C, and E, lower traces). The number of CFs innervating the recorded PC was estimated based on the number of discrete CF-EPSC steps elicited in that PC (*8*, *12*) (Fig. 2, B, D, and F). As reported in (*8*), mGluR1 (−/−) mice had a significantly higher percentage of PCs with multiple CF innervation than the wild-type mice ($P < 0.01$, χ^2 test, Fig. 2, B and D). In contrast, mGluR1-rescue mice had almost the same percentage of PCs with multiple CF innervation as the wild-type mice ($P > 0.05$, χ^2 test, Fig. 2, B and F).

We next determined if LTD at PF-PC synapses would be restored in mGluR1-rescue mice (*13*). In PCs of wild-type mice, conjunctive PF and CF stimulation (CJS) at 1 Hz for 5 min (300 stimuli) resulted in LTD of the initial slope of PF-mediated excitatory postsynaptic potentials (PF-EPSPs) (Fig. 3A), whereas the same protocol did not induce LTD in mGluR1 (−/−) mice (Fig. 3B). In contrast, LTD was induced normally in mGluR1-rescue mice (Fig. 3C).

The cerebellum is implicated in neural mechanisms for interlimb coordination during locomotion (*3*, *14*). We analyzed the temporal relation between the footfall of one limb and that of the other limb during treadmill locomotion (Fig. 4A) (*15*). In wild-type mice, phase intervals between the locomotor

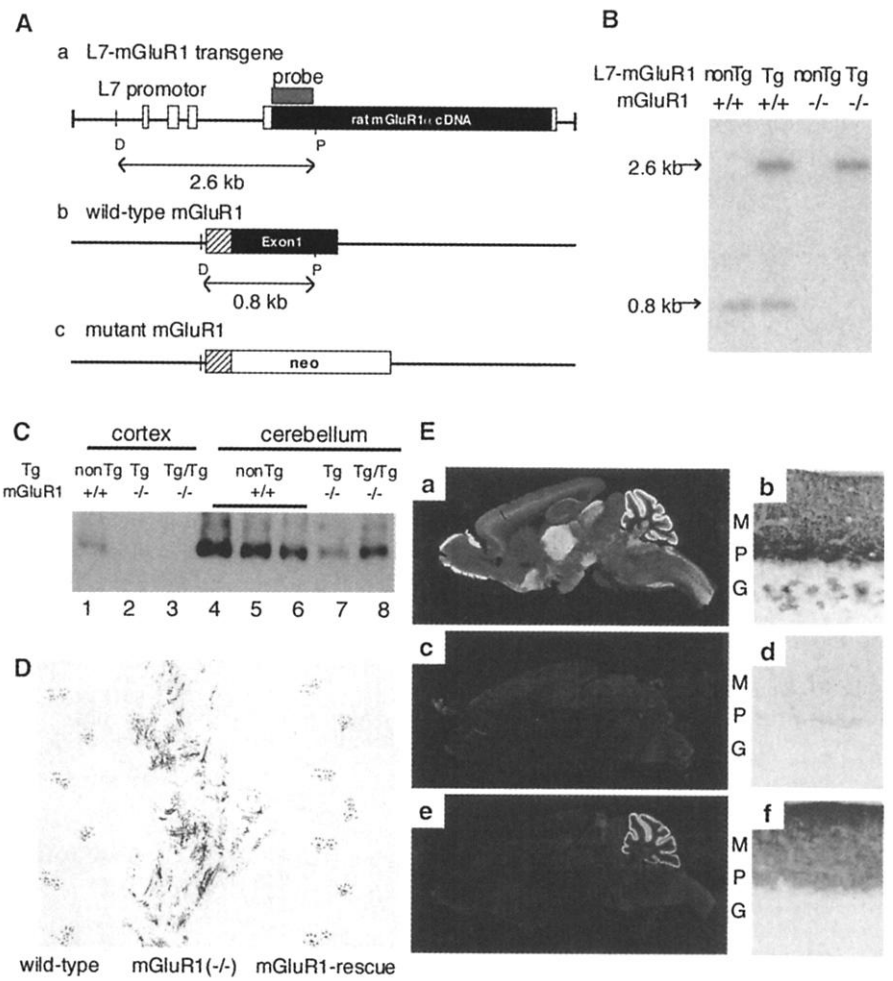

Fig. 1. Generation of L7-mGluR1α transgenic mice and expression of L7-mGluR1α transgene. (**A**) (a) Schematic structure of the transgene construct with the probe for Southern blots. Rat mGluR1α cDNA was inserted into the L7 promoter vector. Open boxes represent exons of the L7 gene (E1 to E4). (b and c) Schematic structure of the wild-type (b) and mutant (c) mGluR1 alleles. Closed and hatched boxes show coding and noncoding regions of the mGluR1 exon, respectively. Numbers signify lengths in base pairs, and the letters indicate restriction sites. D, Dra I; P, Pvu II. (**B**) Southern blot analysis of tail DNA. Genomic DNA was isolated from a litter obtained by breeding mGluR1 (+/−) mice with mGluR1 (+/−) (Tg/+) mice. Endogenous mGluR1 gene and transgene are indicated by the presence of a 0.8-kb and a 2.6-kb Dra I–Pvu II fragment, respectively. (**C**) Total proteins extracted from wild-type, mGluR1-rescue (Tg/+), and mGluR1-rescue (Tg/Tg) cerebral cortices and cerebella were blotted and probed with polyclonal antibodies to mGluR1. Lanes 1, 2, 3, 7, and 8 contained 40 μg of proteins; lanes 4, 5, and 6 contained 4, 2, and 1 μg of proteins, respectively. (**D**) Footprint patterns: mGluR1 (−/−) mice walked with a wide-base rolling motion from side to side. Their steps appeared to be shorter, and their feet tended to sweep along. In contrast, mGluR1-rescue mice could walk a straight line, as did their wild-type littermates. (**E**) Parasagittal sections stained with antibody to mGluR1α, from wild-type (a and b), mGluR1 (−/−) (c and d), and mGluR1-rescue mice (e and f). M, molecular layer; P, Purkinje cell layer; G, granule cell layer.

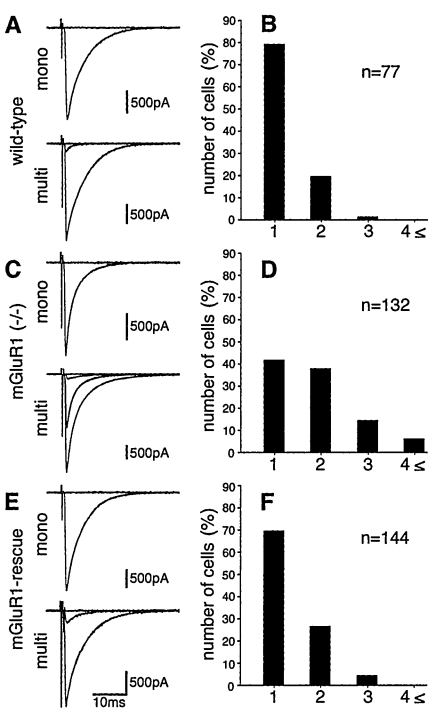

Fig. 2. Normal regression of multiple CF innervation in PCs of mGluR1-rescue mice. (**A**) Sample records of CF-EPSCs from wild-type PCs. One to three traces each were superimposed at threshold intensities. (**B**) Summary graph showing frequency distribution of PCs in terms of the number of discrete steps of CF-EPSCs from wild-type mice. (**C** and **D**) Data from mGluR1 (−/−) PCs. (**E** and **F**) Data from mGluR1-rescue PCs. Numbers of tested PCs: $n = 77$ (from five mice) for (A) and (B), $n = 132$ (from nine mice) for (C) and (D), and $n = 144$ (from nine mice) for (E) and (F).

cycles of two limbs were sharply distributed around 180°, indicating regular alternations of step cycles between two limbs. However, in mGluR1 (−/−) mice there was wide dispersion of phase intervals, suggesting a severe impairment of interlimb coordination. In mGluR1-rescue mice, phase intervals between two limbs were distributed around 180° with a narrow dispersion, indicating that their interlimb coordination was normal. When the belt velocity of the treadmill was increased, the step cycle duration progressively decreased in wild-type and mGluR1-rescue mice (Fig. 4B). However, mGluR1 (−/−) mice did not adapt to change in the belt velocity, and step-cycle durations were different between the fore- and hindlimbs.

mGluR1 (−/−) mice showed a reduction in total walking distance in the open field (*4*). In contrast, we observed no significant differences between wild-type and mGluR1-rescue mice (Fig. 4C) (*16*). Restoration of locomotor activity in mGluR1-rescue mice suggests that the lack of mGluR1 in brain regions other than the cerebellum did not alter the motivational state for locomotion.

To further examine motor coordination, we used the rotating rod task (*17*). Wild-type mice quickly learned how to keep themselves on the rod, whereas mGluR1 (−/−) mice fell off immediately once the rod began to turn (Fig. 4D) (*3*). During any given trial, the average retention time of mGluR1-rescue mice was shorter than that of the wild-type mice (Fig. 4D). However, when we examined the mGluR1-rescue (Tg/Tg) mice, which are homozygous for the L7-mGluR1α transgene and display gene dose-dependent increases in mGluR1α expression (Fig. 1C), they managed to stay on the rod for over 100 s by the fourth trial. There was no significant difference between retention time of wild-type and mGluR1-rescue (Tg/Tg) mice (Fig. 4D). Thus, the level of mGluR1 in PCs appears to be the determining factor for performance of motor coordination on the rotating rod task.

The gene targeting technique is a pertinent and powerful tool to examine the function of a gene in vivo. However, if the gene is expressed in various brain regions or during the course of development, and if there is no regional or temporal restriction in deletion of the gene, it is difficult to attribute the observed abnormality to the lack of the gene product in a specific brain region. Here, we returned the missing mGluR1α only into PC with a PC-specific promoter. The impaired cerebellar CF synapse elimination, deficient LTD, and motor discoordination observed in mGluR1 (−/−) mice were

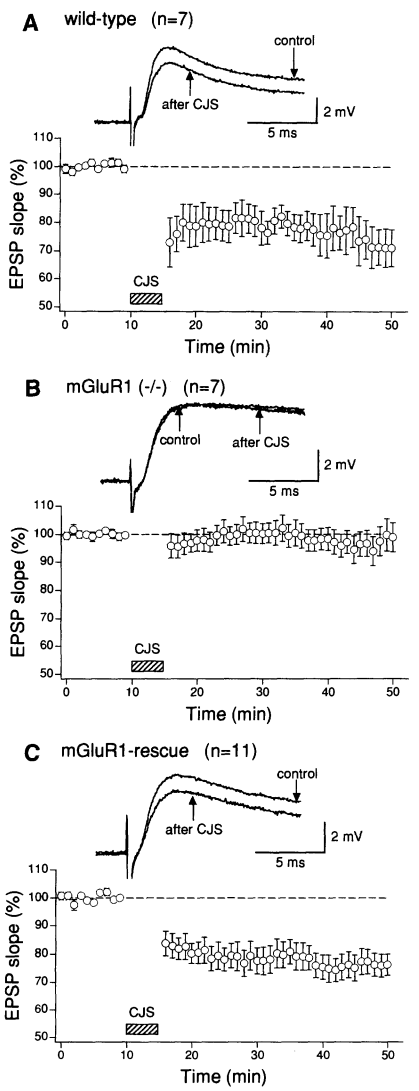

Fig. 3. Normal LTD in PCs of mGluR1-rescue mice. (**A**) In PCs of wild-type mice, conjunctive PF and CF stimulation (CJS) at 1 Hz for 5 min (300 stimuli) resulted in LTD of the PF-EPSP initial slopes (n = 7 from five mice). The data points represent mean ± SEM. Inset shows superimposed PF-EPSP traces recorded before conjunctive stimulation and 30 min after. (**B**) Data obtained from PCs of mGluR1 (−/−) mice (n = 7 from four mice). (**C**) Data from PCs of mGluR1-rescue mice (n = 10 from seven mice).

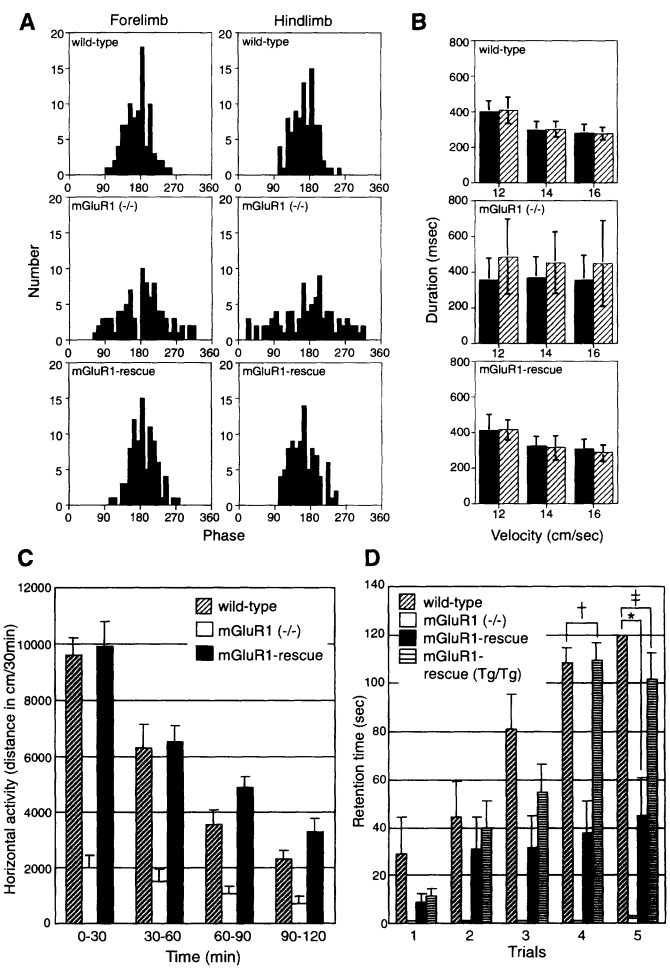

Fig. 4. Interlimb coordination, locomotor activity; and rotating rod test. (**A**) Phase relationships between step cycles of the left and right forelimbs (left) and hindlimbs (right). Data for 90 steps from three mice that were walking on the treadmill at the speed of 14 cm/s. A phase interval of 0° or 360° and that of 180° corresponds to the in-phase and out-phase step cycles, respectively. Variances for both limbs of mGluR1 (−/−) mice were significantly larger than those of two other mouse strains (one-way analysis of variance). (**B**) The step cycle duration of forelimbs (filled columns) and hindlimbs (hatched columns) against different belt velocities. Data (mean ± SD) for 90 steps obtained from three mice. (**C**) Spontaneous locomotor activities in the open field. Horizontal activities in a novel environment for wild-type (n = 7), mGluR1 (−/−) (n = 7), and mGluR1-rescue mice (n = 7) were measured every 30 min over a 2-hour period in daytime with a behavioral tracing analyzer (Muromachi Kikai, Tokyo). Error bars represent SEM (in the first session: wild-type, 9602 ± 635.6 cm; mGluR1-rescue, 9914 ± 892.5 cm; $P > 0.5$, t test, n = 7). (**D**) Rotating rod task. Data represent average of five consecutive trials (maximum retention time, 120 s; rotation speed, 8 rpm). Number of mice examined: n = 10 for wild-type, mGluR1 (−/−), and mGluR1-rescue (Tg/Tg) mice and n = 8 for mGluR1-rescue (Tg/+) mice. Error bars represent SEM. *$P < 0.001$, t test wild-type versus mGluR1-rescue (Tg/+) mice; †$P > 0.9$ and ‡$P > 0.1$, t test wild-type versus mGluR1-rescue (Tg/Tg) mice.

all restored. Our results indicate that mGluR1 in PCs is essential for these three events and suggest that mGluR1 in PC is a key molecule needed for normal development and function of the cerebellum. A rescue experiment with tissue-specific promoter is a most productive approach to specify the brain region or cell type responsible for the phenotype observed in conventional knockout mice.

References and Notes

1. M. Masu *et al.*, *Nature* **349**, 760 (1991); S. Nakanishi, *Science* **258**, 597 (1992); N. Okamoto *et al.*, *J. Biol. Chem.* **269**, 1231 (1994); S. Nakanishi, *Neuron* **13**, 1031 (1994).
2. A. Aiba *et al.*, *Cell* **79**, 365 (1994).
3. A. Aiba *et al.*, *Cell* **79**, 377 (1994).
4. F. Conquet *et al.*, *Nature* **372**, 237 (1994).
5. P. Sillevis Smitt *et al.*, *N. Engl. J. Med.* **342**, 21 (2000).
6. J. P. Changeux, P. Courrege, A. Danchin, *Proc. Natl. Acad. Sci. U.S.A.* **70**, 2974 (1973); F. Crepel, *Trends Neurosci.* **5**, 266 (1982); J. Mariani and N. Delhaye-Bouchaud, *News Physiol. Sci.* **2**, 93 (1987).
7. M. Ito, *The Cerebellum and Neural Control* (Raven Press, New York, 1984).
8. M. Kano *et al.*, *Neuron* **18**, 71 (1997); C. Levenes, H. Daniel, D. Jaillard, F. Conquet, F. Crepel, *Neuroreport* **8**, 571 (1997).
9. We generated transgenic mice (L7-mGluR1) that expressed mGluR1α under the control of the PC-specific L7 promoter [J. Oberdick, R. J. Smeyne, J. R. Mann, S. Zackson, J. I. Morgan, *Science* **248**, 223 (1990); R. J. Smeyne *et al.*, *Science* **254**, 719 (1991); R. J. Smeyne *et al.*, *Mol. Cell. Neurosci.* **6**, 230 (1995)]. A 3.7-kb Sac II–Fsp I fragment of rat mGluR1α cDNA containing a 26 base pair (bp) 5′ untranslated region (UTR), a 3597-bp coding region, and a 36-bp 3′ UTR was introduced into exon 4 of the L7 gene cassette. We obtained eight independent L7-mGluR1 transgenic founder mice by microinjecting the transgene into the pronuclei of fertilized mGluR1 (+/−) eggs. The mGluR1-rescue mice were obtained by breeding mGluR1 (+/−) with transgenic mice. The cerebellum-restricted expression of the transgene was examined by Western blotting with polyclonal antibodies to rat mGluR1 (Upstate Biotechnology, Lake Placid, NY). One line expressed the L7-mGluR1α transgene in the cerebellum but not in the cerebral cortex.
10. Adult wild-type, mGluR1 (−/−), and mGluR1-rescue (Tg/+) mice were deeply anesthetized with pentobarbital (100 mg/kg of body weight) and were perfused transcardially with 3.5% paraformaldehyde, 0.05% glutaraldehyde, and 1% picric acid in 0.1 M sodium phosphate buffer (pH 7.3). The brains were cryoprotected with 25% (w/w) sucrose in 0.1 M phosphate buffer overnight at 4°C and cut on a freezing microtome or cryostat into 40-μm-thick parasagittal sections. The free-floating sections were incubated overnight at room temperature with antibodies to mGluR1α (1.0 μg/ml) [R. Shigemoto *et al.*, *Nature* **381**, 523 (1996)], 0.1% Triton X-100, and 0.25% carrageenan. These sections were then washed with phosphate buffered saline (PBS), incubated with biotinylated antibody to guinea pig immunoglobulin G, washed again, and reacted with avidin-biotin-peroxidase complex (ABC Kit, Vector, Burlingame, CA). Finally, the sections were reacted with 0.02% diaminobenzidine tetrahydrochloride and 0.002% hydrogen peroxide in 50 mM tris-HCl (pH 7.6).
11. Parasagittal cerebellar slices (250 μm thick) were prepared from wild-type, mGluR1 (−/−), and mGluR1-rescue mice, as described [I. Llano, A. Marty, C. M. Armstrong, A. Konnerth, *J. Physiol.* **434**, 183 (1991)]. Whole-cell recording was made from visually identified PCs with either an Olympus (BH-2, Tokyo, Japan) or Zeiss (Axioskop, Oberkochen, Germany) upright microscope [F. A. Edwards, A. Konnerth, B. Sakmann, T. Takahashi, *Pflügers Archiv. (Eur. J. Physiol.)* **414**, 600 (1989)]. Resistance of patch pipettes was 3 to 6 megohm when filled with an intracellular solution composed as follows: 60 mM CsCl, 30 mM Cs D-gluconate, 20 mM tetraethylammonium-Cl (TEA-Cl), 20 mM BAPTA [1,2-bis(2-aminophenoxy)ethane-*N*,*N*,*N*′,*N*′-tetraacetic acid (a Ca^{2+} buffer)], 4 mM $MgCl_2$, 4 mM adenosine triphosphate (ATP), and 30 mM Hepes, pH 7.3 (adjusted with CsOH). The pipette access resistance was compensated. The standard bathing solution was composed as follows: 125 mM NaCl, 2.5 mM KCl, 2 mM $CaCl_2$, 1 mM $MgSO_4$, 1.25 mM NaH_2PO_4, 26 mM $NaHCO_3$, and 20 mM glucose, which was bubbled continuously with a mixture of 95% O_2 and 5% CO_2. Bicuculline (10 μM) was included to block spontaneous inhibitory postsynaptic currents. Membrane currents were recorded with an Axopatch-1D amplifier (Axon Instruments, Foster City, CA). Glass pipettes filled with standard extracellular solution were used to stimulate CFs in the granule cell layer. The PULSE software (version 8.2, HEKA, Lambrecht, Germany) was used for stimulation and data acquisition. The signals were filtered at 3 kHz and digitized at 20 kHz.
12. M. Kano *et al.*, *Cell* **83**, 1223 (1995); S. Offermanns *et al.*, *Proc Natl. Acad. Sci. U.S.A.* **94**, 14089 (1997); M. Kano *et al.*, *Proc Natl. Acad. Sci. U.S.A.* **95**, 15724 (1998).
13. To measure LTD, a potassium-based intracellular solution was used. The composition was as follows: 70 mM KCl, 60 mM K D-gluconate, 4 mM $MgCl_2$, 4 mM ATP, 0.4 mM guanosine triphosphate (GTP), and 30 mM Hepes, pH 7.3 (adjusted with KOH). EPSPs elicited by PF stimulation were recorded with an Axoclamp-2B amplifier (Axon Instruments). The membrane potential was kept constant at −70 to −80 mV by injecting hyperpolarizing currents (200 to 500 pA).
14. G. N. Orlovsky, F. V. Severin, M. L. Shik, *Biofizika* **11**, 509 (1966); J. A. Gruner, J. Altman, N. Spivack, *Exp. Brain Res.* **40**, 361 (1980); M. Udo, K. Matsukawa, H. Kamei, Y. Oda, *J. Neurophysiol.* **44**, 119 (1980); P. A. Fortier, A. M. Smith, S. Rossignol, *Exp. Brain Res.* **66**, 271 (1987); N. Kashiwabuchi *et al.*, *Cell* **81**, 245 (1995); L. Chen, S. Bao, J. M. Lockard, J. K. Kim, R. F. Thompson, *J. Neurosci.* **16**, 2829 (1996).
15. Mice were placed under pentobarbital anaesthesia (40 to 50 mg/kg of body weight) before surgical operation. A platform for fixation of the head to a stereotaxic frame was built in aseptic conditions. After making an incision in the skin, four small screws around the central long bolt were mounted on the parietal cranium, and were sealed by dental cement. Cinematographic recordings were started 2 to 4 days after the surgery. During recordings, a mouse was mounted on the treadmill with its head fixed, but its body and limbs were not restrained. Locomotion was induced by moving the belts at moderate velocities (12, 14, and 16 cm/s). Movement of the mice was filmed with a video camera (SONY DXC-107A, Tokyo, Japan) equipped with a shutter operating at 60 fields per second. A field-by-field analysis (16.7-ms time resolution) of the videotapes revealed the temporal measurements.
16. Animals were housed at 21° ± 1°C with free access to food and water and tested at 12 to 15 weeks. Experiments were conducted in accordance with ethical guidelines of the Institute of Medical Science, University of Tokyo. In the open-field test, each mouse was placed in the middle of a 75-cm-diameter enclosure, and the walking route of the mouse was traced with a behavioral tracing analyzer (Muromachi Kikai, Tokyo). The total walking distance was recorded every 30 min over a 2-hour period.
17. The Rota-Rod Treadmill (Muromachi Kikai) consists of a gritted plastic rod (3 cm in diameter, 10 cm long) flanked by two large round plates (50 cm in diameter). The time the mouse remained on the rod was measured. A maximum of 120 s was allowed to test each animal.

18. We thank S. Nakanishi for rat mGluR1α cDNA. Supported in part by Grants-in-Aid for Scientific Research from the Ministry of Education, Science, Sports and Culture of Japan (to M.K. and A.A.); the Grant-in-Aid for Special Scientific Research on Agriculture, Forestry, and Fisheries (to A.A); the Human Frontier Science Program (to M.K.); and by the Special Coordination Funds for Promoting Science and Technology from Science and Technology Agency of Japan (to M.K.). Language assistance was provided by M. Ohara.

12 January 2000; accepted 13 April 2000

Dissociating the Role of the Dorsolateral Prefrontal and Anterior Cingulate Cortex in Cognitive Control

Angus W. MacDonald III,[1] Jonathan D. Cohen,[2,4] V. Andrew Stenger,[3] Cameron S. Carter[1,2]*

Theories of the regulation of cognition suggest a system with two necessary components: one to implement control and another to monitor performance and signal when adjustments in control are needed. Event-related functional magnetic resonance imaging and a task-switching version of the Stroop task were used to examine whether these components of cognitive control have distinct neural bases in the human brain. A double dissociation was found. During task preparation, the left dorsolateral prefrontal cortex (Brodmann's area 9) was more active for color naming than for word reading, consistent with a role in the implementation of control. In contrast, the anterior cingulate cortex (Brodmann's areas 24 and 32) was more active when responding to incongruent stimuli, consistent with a role in performance monitoring.

Cognitive control has long attracted the attention of philosophers and psychologists interested in how the human brain carries out the higher functions of awareness, memory, and language. The concept of control generally refers to a resource-limited system that guides voluntary, complex actions. Solving difficult, novel, or complex tasks, overcoming habitual responses, and correcting errors all require a high